Published in final edited form as:
Reproduction. 2014 ; 147(1): . doi:10.1530/REP-13-0354.

Effects of the Use of Assisted Reproduction and High Caloric Diet Consumption on Body Weight and Cardiovascular Health of Juvenile Mouse Offspring

Angela L. Schenewerk[1], **Francisco Ramírez**[2], **Christopher Foote**[2], **Tieming Ji**[3], **Luis A. Martínez-Lemus**[*,2,4,5], and **Rocío Melissa Rivera**[*,1]

[1]Division of Animal Sciences, University of Missouri, Columbia, MO

[2]Dalton Cardiovascular Research Center, University of Missouri, Columbia, MO

[3]Department of Statistics, University of Missouri, Columbia, MO

[4]Department of Biological Engineering, University of Missouri, Columbia, MO

[5]Department of Medical Pharmacology and Physiology, University of Missouri, Columbia, MO

Abstract

Maternal obesity and the use of assisted reproductive technologies (ART) are two suboptimal developmental environments that can lead to offspring obesity and cardiovascular disease. We hypothesized that these environments independently and synergistically adversely affect the offspring's weight and cardiovascular performance at ∼7 weeks of age. Mice were fed either 24% fat and 17.5% high fructose corn syrup (HF) or maintenance chow (5% fat; LF). Dams were subdivided into no-ART and ART groups. ART embryos were cultured in Whitten's medium and transferred into pseudopregnant recipients consuming the same diet as the donor. Offspring were fed the same diet as the mother. Body weights (BW) were measured weekly and mean arterial pressure (MAP) was collected through carotid artery catheterization at sacrifice (55 ± 0.5 days old). Expression of genes involved in cardiovascular remodeling was measured in thoracic aorta using qRT-PCR, and levels of reactive oxygen species were measured intracellularly and extracellularly in mesenteric resistance arteries. ART resulted in increased BW at weaning. This effect decreased over time and diet was the predominant determinant of BW by sacrifice. Males had greater MAP than females ($p=0.002$) and HF consumption was associated with greater MAP regardless of sex ($p<0.05$). Gene expression was affected by sex ($p<0.05$) and diet ($p<0.1$). Lastly, the use of ART resulted in offspring with increased intracellular ROS ($p=0.05$). In summary, exposure to an obesogenic diet pre- and/or post-natally affects weight, MAP, and gene expression while ART increases oxidative stress in mesenteric resistance arteries of juvenile offspring, no synergistic effects were observed.

Introduction

Developmental priming and fetal programming have emerged as important hypotheses that partly explain the surge in obesity and cardiovascular disease (CVD) currently observed

[*]Correspondence should be addressed to R.M. Rivera; 164 Animal Science Research Center, 920 East Campus Drive, University of Missouri, Columbia, MO 65211; riverarm@missouri.edu or to L.A. Martinez-Lemus; Department of Medical Pharmacology and Physiology, Dalton Cardiovascular Research Center, University of Missouri-Columbia, 134 Research Park Drive, Columbia, MO 65211;martinezlemusl@missouri.edu.

Declaration of interest
None declared.

worldwide (WHO 2013a, WHO 2013b). These hypotheses, collectively known as developmental origins of adult disease, assert that the uterine environment has profound effects on the body composition and cardiovascular performance of the offspring in later life (Hales 1992, Lawlor *et al*. 2004).

Recent research has shown that maternal obesity, over-nutrition, and diabetes increase the incidence of glucose intolerance, arterial endothelial dysfunction, arterial stiffness, hypertension, and CVD in the offspring in humans and mice (Wildman *et al*. 2003, Samuelsson *et al*. 2008, Samuelsson *et al*. 2010, Kelsall *et al*. 2012, Torrens *et al*. 2012, Magliano *et al*. 2013). In mice, maternal obesity can result in progenies with increased body weight (Samuelsson *et al*. 2008, Franco *et al*. 2012, Magliano *et al*. 2013). Further, Torrens *et al*. showed that offspring exposed to maternal obesity had decreased production of the vasodilator nitric oxide (NO) , a blunted vasodilatory response to acetylcholine in the femoral artery, as well as increased systolic blood pressure at 30 weeks of age (Torrens *et al*. 2012). Maternal high caloric intake in mice has also been linked to impaired vascular responses and increased blood pressure of the offspring during adulthood (Samuelsson *et al*. 2008).

The use of Assisted Reproductive Technologies (ART) has been associated with adverse outcomes in children (Olson *et al*. 2005, Kallen *et al*. 2010, Wen *et al*. 2010). Studies have shown that the use of *in vitro* fertilization (IVF) results in an increased risk for congenital malformations such as cardiac septal defects, neural tube defects and cleft palate (Olson *et al*. 2005, Reefhuis *et al*. 2009, Kallen *et al*. 2010). In addition, Wen *et al*. found that the risk for congenital heart defects with the use of ART was amplified when the mother was obese (Wen *et al*. 2010).

Retrospective studies in human (Wikstrand *et al*. 2008, Ceelen *et al*. 2009, Sakka *et al*. 2010) have also pointed at the method of conception as a causative factor for abnormal cardiovascular parameters in children during postnatal development. For example, it has been demonstrated that children conceived by the use of ART have increased systolic and diastolic blood pressure, increased vascular dysfunction, and decreased retinal vascular branching (Ceelen *et al*. 2008, Wikstrand *et al*. 2008, Sakka *et al*. 2010, Scherrer *et al*. 2012). Similarly, in mice, an association exists between ART and an elevated systolic blood pressure (Watkins *et al*. 2007). Further, increased angiotensin converting enzyme (ACE), which cleaves angiotensin I into the vasoconstrictor angiotensin II, has also been observed in mice offspring conceived via ART (Watkins *et al*. 2007). Lastly, the use of ART has been associated with increased adiposity in children (Ceelen *et al*. 2007, Belva *et al*. 2012). For example, children conceived by IVF and ICSI have higher levels of peripheral adiposity than age matched naturally conceived controls at 8–18 years of age (Ceelen *et al*. 2007, Belva *et al*. 2012).

Cardiovascular disease is the number one cause of death. In 2008 CVD accounted for 30% of deaths worldwide (WHO 2013b). Obesity and hypertension are two important contributors to the high incidences of CVD mortality worldwide (WHO 2013b). The development of hypertension has been proposed to involve the matrix metalloproteinases (MMPs) and reactive oxygen species [ROS;(Martinez-Lemus & Galinanes 2011)]. ROS can mediate the expression and activation of MMPs (Siwik *et al*. 2001, Martinez-Lemus *et al*. 2011, Zhang *et al*. 2013). In the vasculature, ROS are mainly produced by the enzyme NADPH oxidase [NOX; (Cai *et al*. 2003)]. MMPs are involved in processes such as the degradation of the extracellular matrix (ECM), the cleavage of extracellular receptors (Rodrigues *et al*. 2010), disruption of cellular adhesions (Yang *et al*. 2007) and shedding of vasoactive factors within the ECM (Hao *et al*. 2004). Specifically, MMP2 and MMP9 have been implicated in vascular remodeling, and MMP7 might also be involved as it appears to

play a role in hypertension (Lehoux *et al*. 2004, Wang *et al*. 2009, Martinez-Lemus *et al*. 2011). Tissue Inhibitors of MMPs (TIMPs) are endogenous inhibitors of the MMPs, and an imbalance between TIMPs and MMPs has been implicated in pathological conditions (Gomez *et al*. 1997).

Maternal obesity and the use of ART often coincide because many women of reproductive age face infertility, and the number of them who attend ART clinics is rising (Robker 2008). It is clear that obesity and ART are each predisposing children to CVD. However, given the short history of the use of ART, no studies have yet addressed the threat of CVD from the combination of the two suboptimal maternal environments, despite the large number of children who have been exposed to it. In the current study we hypothesize that obesity and ART independently and synergistically adversely affect the cardiovascular health and body weight of the offspring. We further hypothesize that these two suboptimal developmental environments are associated with higher blood pressure in the offspring, and that this is associated with expression of the MMPs, TIMPs and NOXs in the vasculature. To test these hypotheses, two suboptimal developmental environments were used; namely, those that exist with an obesogenic environment and with the use of ART. We sought to determine what effect these two environments, either alone or in combination, would have on cardiovascular health markers in juvenile mice offspring (∼7 weeks of age). The measures of cardiovascular health chosen in this study were MAP, the expression of genes implicated in poor cardiovascular health and vascular remodeling (*Mmp2*, *Mmp9*, *Timp1*, and *Nox2*), and levels of intracellular and extracellular ROS. We also measured offspring body weight weekly until sacrifice, as high body weight has been associated with adverse cardiovascular outcomes (NIH 2012).

Materials and Methods

Animals

All animal procedures were approved by the Institutional Animal Care and Use Committee of the University of Missouri under protocol number 7501. The strain of the females used for this experiment was NSA (CF1; Harlan Laboratories, Indianapolis, IN, USA) while the strain of the studs and vasectomized males was B6D2F1/J (The Jackson Laboratory, Bar Harbor, ME, USA). Females were between 6 and 10 weeks of age, and were housed under 12 hour (h) light/dark cycle between 20°C and 23.3°C in groups until conception when they were individually caged. Mice were given *ad libitum* access to water and the appropriate diet.

Diet

Experimental animals were fed either a “high fat, high fructose” (HF) or “low fat, no fructose” (LF) diet. The HF group were fed a diet containing 24% fat and 17.5% high fructose corn syrup from TestDiet 58Y1 (TestDiet ; St. Louis, MO, USA) *ad libitum*. The calories (kcal%) provided by the HF diet are as follows: protein = 17.6%, carbohydrate = 36% and fat = 46.4%. The females in the LF group were fed a diet containing 5% fat (measured by ether extraction; Lab Diets 5001 PMI Nutritional International St. Louis, MO, USA) *ad libitum*. The calories (kcal%) provided by the LF diet is a follows: protein = 28.5%, carbohydrate = 58% and fat = 13.5%. The LF females were given Lab Diet 5008 (6.5% fat) during pregnancy and lactation. The calories (kcal%) provided by the LF pregnancy diet are as follows: protein=26.8%, carbohydrate=56.4% and fat=16.7%. The HF diet administered prior to and during pregnancy and lactation was TestDiet 58Y1 (46% kcal fat with corn syrup). Note: the terms “maternal and offspring consumption of HF diet” and “exposure to an obesogenic diet” will be used interchangeably.

Control (no ART) groups

The control females were fed the HF or LF diet at least 3 weeks prior to being paired with proven fertility B6D2F1/J males. Three weeks were chosen because this is the approximate time required for oocyte development in mice (Eppig *et al*. 2002). Copulation was confirmed by visual observation of a copulatory plug. Pregnant females were placed in a separate cage and were allowed to carry the pregnancy to term. Twelve total control females were paired with fertile males (6 HF and 6 LF), but one HF female did not become pregnant. After birth, the litters were culled to 8 pups (4 males and 4 females, when possible), to help control for the smaller litter sizes in the ART groups.

Assisted Reproduction groups

Three ART procedures were used in this experiment, namely, superovulation, embryo collection and culture, and embryo transfer in order to simulate three procedures commonly used in human ART.

Superovulation—Females of 6–10 weeks of age fed either HF or LF diet for three weeks before superovulation received an intraperitoneal (IP) injection of 5 IU equine chorionic gonadotropin (eCG; Calbiochem La Jolla, CA, USA) followed by 5 IU of human chorionic gonadotropin (hCG; Sigma St. Louis, MO, USA) 45 h later. The injections were given to increase the number of oocytes ovulated by each animal. Superovulated females were then co-caged overnight with B6D2F1/J intact males.

Embryo Collection and Culture—Two-cell embryos were harvested from the oviduct approximately 46 h post-hCG injection. Oviducts were flushed with warm bicarbonate-free minimal essential medium (Earle's salt) supplemented with 3 mg/ml polyvinylpyrrolidone (PVP) and 25 mM Hepes (MEM+PVP [pH 7.3]; Sigma St. Louis, MO, USA). Embryos were washed from debris with three consecutive washes in MEM+PVP and once in Whitten's medium. Whitten's medium was prepared as previously published by us (Negron-Perez *et al*. 2013). Whitten's medium has previously been shown to support development to term (Ecker *et al*. 2004, Sommovilla *et al*. 2005), although it is known to be a suboptimal culture medium (Rinaudo & Schultz 2004). We purposely used this medium to determine whether the cardiovascular measures examined in the current study would be adversely affected by a suboptimal culture medium, as such findings could direct the focus of future studies in more favorable culture media. The embryos were cultured at 37°C in Whitten's medium in an atmosphere of 5% CO_2 in air at a density of 1 embryo per ~3.5 μl of medium. Embryos were cultured for 3 days (or 116 h post-hCG) at which time zona-enclosed blastocysts were transferred to the uteri of day 2.5 (d2.5) pseudopregnant NSA (CF1) females.

Embryo Transfers—Females designated as embryo recipients [NSA(CF1)] were fed HF or LF diets at the same time as the embryo donors prior to receiving the superovulation protocol described above. Immediately after the hCG injection, the females were co-caged overnight with vasectomized B6D2F1/J males. Females which showed a copulatory plug the following morning (denoted as d0.5 of pseudopregnancy) were selected as potential embryo recipients. A plane of anesthesia was reached by an IP injection of the 2.5% (w/v) Avertin stock at 0.014 ml/g body weight (Nagy A 2003). Twenty blastocyst-stage embryos produced as described above were transferred (ten/uterine horn) to embryo recipients on d2.5 of pseudo-pregnancy according to standard procedures (Nagy A 2003). Pseudopregnant recipients were consuming the same diet as the embryo donor. Pregnant recipients were returned to their cages and allowed to carry their pregnancies to term. Forty-five transfers were performed (22 LF and 23 HF). Nearly 27% of transfers resulted in pregnancy (determined by birth of offspring; Supplementary Table 1).

Pregnancy, lactation and weaning

All females were maintained on the diet they had been consuming prior to becoming pregnant until their role in the experiment was completed at weaning. Offspring were weaned from the mothers at 22 days post-partum. They were separated by sex and placed on the same diet that the mothers had consumed until sacrifice.

Measurement of offspring body weights

Body weight was recorded using a standard scale (Mettler Toledo; Columbus, OH, USA) five days after birth, and every week thereafter until sacrifice. Control litters were culled to eight (4 males and 4 females when possible) at the 5-day weighing to control for the larger litter sizes in the control groups. No identification marks were used prior to weaning; therefore, weights were recorded separately for males and females from each litter and averaged each week during the first three weeks. Each individual received an identifying ear punch at weaning, and weights were recorded by individual from that point on.

Mean arterial pressure measurement

Offspring male (n=37) and female (n=31) mice 55.5 ± 0.5 (n=68) days old were anesthetized by inhalation of 5% isoflurane until visible loss of consciousness. At that point, mice were placed in dorsal recumbency and maintained under anesthesia at 3% (v/v) through a cone covering the nose and mouth until surgical plane anesthesia was confirmed by loss of spinal reflexes. The right carotid artery was cannulated with a polyethylene catheter (PE-10) filled with phosphate-buffered physiological saline solution containing 100 U/mL of heparin. The catheter was connected to a pressure transducer in order to measure mean arterial pressure (MAP) with the use of a PowerLab 4/30 Data Acquisition System (ADInstruments Colorado Springs, CO,USA). Following catheterization, the level of anesthesia was lowered to 2% (v/v) for 10 min., and the average systolic and diastolic pressures recorded during the final minute were used to calculate MAP. It should be noted that three animals had bleeding during catheterization, and were excluded from the MAP analysis as blood loss can affect pressure.

Mesenteric resistance artery and thoracic aorta collection

Subsequent to MAP measurement, animals were euthanized under anesthesia. A portion of the mesentery was excised and pinned flat in a refrigerated (4 °C) dissecting chamber containing physiological saline solution (PSS) of the following composition (in mmol/L): 145.0 NaCl, 4.7 KCl, 2.0 $CaCl_2$, 1.2 $MgSO_4$, 1.0 NaH_2PO_4, 5.0 dextrose, 3.0 3-(N-morpholino) propanesulfonic acid (MOPS) buffer, 2.0 pyruvate, 0.02 EDTA, and 0.15 bovine serum albumin (BSA), pH 7.4. Small pieces (∼3mm length) of second order mesenteric resistance arteries were isolated and stored at −70°C for subsequent analysis of ROS using high performance liquid chromatography (HPLC). A small section (∼5mm length) of the thoracic aorta was also collected and stored at −70°C for quantitative RT-PCR analysis. Due to time constraints for the processes performed, tissues were only collected for two animals per day. In order to keep the age average similar between the ART and No ART groups, 34 of the 36 ART offspring and 34 of the 87 No ART controls were collected and used for the remainder of the study. The collected offspring were selected to have at least one male and one female for each mother. Two or three offspring were collected from all of the control females except for the last LF control female (three males and three females were collected) and the last two HF control females (two males and two females were collected). All ART-conceived pups were collected except for two HF males who had advanced too far in age by the time of collection.

Dihydroethidium incubation of single mesenteric resistance arteries for detection of ROS

Isolated pieces of mesenteric resistance arteries were taken from the −70°C freezer, placed in 99 μL 1x phosphate buffered saline (PBS; 137 mM NaCl, 2.7 mM KCl, 10 mM Na_2HPO_4, 1.8 mM KH_2PO_4) with 100 μM DTPA (Sigma-Aldrich St. Louis, MO, USA) and incubated in a 37°C water bath for 10 min. The 100 μM DTPA was prepared as previously described (Buettner 2008). Briefly, 0.1967 g DTPA was added to 1.7 mL 1M NaOH to make the DTPA go into solution more easily. The flask was then filled to approximately 40 mL with ultrapure H_2O. The solution was sonicated to bring the DTPA into solution. Then, the solution was adjusted to a pH of 7.1 using a 1M HCl solution before bringing the solution to a final volume of 50mL with ultrapure H_2O. A 5 mM stock solution of dihydroethidium (DHE) was made by dissolving 1 mg DHE (Molecular Probes-Life Technologies Grand Island, NY, USA) in 634 μL DMSO (Sigma St. Louis, MO, USA). The resulting solution was separated into 15 μL aliquots and lyophilized for 2 h. The lyophilized DHE aliquots were stored at −20°C until use. On each day of the experiment, the lyophilized DHE was resuspended in 15 μL pure HPLC grade acetonitrile. After the initial incubation, 1 μL of a 5 mM DHE stock in acetonitrile was added to the solution bathing the vessel to bring the final concentration to 50 μM DHE. Ambient light was avoided to diminish excess oxidation of the DHE. The resistance artery was incubated with DHE at 37°C in the water bath for 1h, with gentle agitation every 10 min. The vessel was then removed and washed twice, consecutively, in 400 μL 1xPBS.

Fluorescence confocal microscopy for detection of intracellular ROS

After being washed in 1xPBS, the vessels were placed on a glass slide in a drop of 1xPBS and covered with a 1.5 thickness coverslip. Two random areas were chosen to be imaged for each vessel. Images were obtained using a Leica True Confocal Scanning-Spectral Photometric 5 DMI 6000 Confocal Laser Scanning Microscope (Leica TCS SP5). A 3D image was obtained for each section at a photomultiplier gain of 800 V using a 20x dry lens. DHE was detected using a multi-photon excitation of 800 nm and an emission detection in the range of 600–700 nm. DHE has previously been used to detect superoxide in arterioles (Martinez-Lemus *et al*. 2011), as it forms a red fluorescent product upon oxidation (Owusu-Ansah *et al*. 2008). Laser scanning was performed using a resonator set at 8000 Hz to reduce photo bleaching. Z-sections were set at 0.5 μM to cover the entire vessel. All images were taken at the same excitation power and detection perameters. Analysis of relative DHE fluorescence was performed using Imaris 7.6.1 software over an area of 150×150×20 pixels for each vessel. Values for DHE fluorescence were averaged over the two areas of the vessel that were imaged. Readings for intracellular ROS were excluded if there was discrepancy in the relative DHE fluorescence between the two areas on the vessel from the same individual.

High performance liquid chromatography (HPLC)

HPLC was performed using 50 μL of the original DTPA+1xPBS+DHE solution used to bathe the resistance artery in order to detect the oxidation of DHE outside the cells, which is a measure of extracellular ROS production. A C8 reverse phase column (Phenomenex Torrence, CA, USA) was used to separate the two byproducts of DHE oxidation, 2-hydroxyethidium (2-OH-Et) and ethidium (Et). The phase solutions used for product separation were Solution A (ultrapure water), Solution B (99.9% v/v water with 0.1% v/v TFA), and Solution C (99.9% v/v acetonitrile with 0.1% v/v TFA; Fischer Pittsburgh, PA, USA). The samples were placed in a Waters 2590 Separation Module and 2-OH-Et and Et fluorescence were detected using a Waters 474 Scanning Fluorescence detector set at an excitation of 510 nm and emission of 595 nm. Each day before running samples, the column was cleaned by running 99.9% v/v acetonitrile with 0.1% v/v TFA for 20 min. at a flow of 1 ml/min., followed by 100% ultrapure water at a flow of 0.5 ml/min. for 20 min. This

cleaning was repeated after every 4 or 5 samples to stop the pressure in the column from increasing. For each sample being run, a gradient of acetonitrile (v/v) in water was used to elute the samples. The gradient was run at a flow of 0.4 ml/min. with an increase in acetonitrile from 10% to 46% in the first 10 min., an increase again to 100% from min. 20 to 25, and ending with the original 10% acetonitrile from 25 to 35 min. to clean the column. The 2-OH-Et eluted at 16.19 ± 0.03 min. and the Et eluted at 16.61 ± 0.03 min. (See Fig. 4A for a representative example). The Empower program (Waters, Build #1154) was used to extract the areas under the 2-OH-Et and Et peaks detected by the fluorescence detector. One vessel for a LF No ART control male was lost during transfer to the DHE incubation step, so this observation is not included.

Homogenizing vessels for protein measurement

An Omni Bead Ruptor 24 Homogenizer (Omni International Kennesaw, GA, USA) was used to pulverize the resistance arterioles. After the confocal image was taken, the vessels were placed in a 0.5mL tube with a cap (Omni International Kennesaw, GA, USA) with 100 μL pure HPLC grade acetonitrile and 50 mg of 0.1 mm glass beads (Omni International Kennesaw, GA, USA). The program for homogenization was performed at 22°C. There were 3 cycles, each at a speed of 8 m/s for 45 sec., with a 3 sec. wait time between cycles. The tubes were centrifuged briefly after homogenization to ensure the beads were at the bottom of the tube, and 60 μL of the supernatant was recovered. This supernatant was sonicated for 1 min. to further lyse the tissue. Then, the solution was centrifuged at 2000xg for 10 min., and 50 μL of the supernatant was removed. The remaining 10 μL was used for protein measurement using a Micro BCA Kit.

Protein assays using MicroBCA kit

Each sample was diluted 1:4 (v/v) in pure HPLC grade acetonitrile (Fischer Pittsburgh, PA, USA) prior to protein detection. The Micro BCA™ Protein Assay Kit (Pierce Rockford, IL, USA) was used to detect the concentration of protein for each sample. A standard curve with bovine serum albumin (BSA) was generated using a blank (pure acetonitrile) and the concentrations from 1 μg to 200 μg/mL in acetonitrile. The working reagent was prepared in accordance with manufacturer's instructions. Reactions were prepared by mixing 4 μL of the BSA standard or diluted sample with 4 μL of the working reagent. The reactions were incubated at 60°C for 1 h, and then allowed to cool to room temperature. A Nanodrop spectrophotometer was used to measure the absorbance of each sample at 562 nm. A standard BSA curve was performed each day, and the sample absorbances were plotted against the standard curve to determine the concentration in μg/mL.

RNA extraction from thoracic aorta and RT-PCR

RNA isolation was performed on thoracic aorta segments using the DynaBEADS mRNA DIRECT KIT (Invitrogen, Grand Island, NY, USA). The DynabeadOligo (dT)25 beads were equilibrated according to the manufacturer's instructions. For RNA and DNA isolation, thoracic aorta segments were placed in 200 μL lysis buffer (100 mM Tris-HCl, 500 mM LiCl, 10 mM EDTA, 1% LiDS, 5 mM dithiothreitol), pulverized with a DNase-RNase free pestel and then sheared by passing through a 20 gauge needle followed by a 22 gauge needle. Isolation of mRNA separated from the beads was then performed following manufacturer's specifications. The final wash of the beads was performed in 20 μL sterile water, and then heated at 80°C for 2 min. to separate the mRNA from the beads. The water with the mRNA was quickly removed from the beads, and 3 μL was used for the creation of a 60 μL cDNA reaction using 100 U Superscript II Reverse Transcriptase (Invitrogen, Grand Island, NY, USA) and the following (1X First-Strand Buffer, 10 mM DTT, 0.8 mM dNTPs, 0.5 μg random primers, 44 U RNasin). The reaction was incubated at 42°C for 1 h followed by 95°C for 10 min. One microliter of the resulting cDNA was used for each qRT-PCR

reaction. Procedures were followed using manufacturer's instructions, thus a template quantification step was not used.

Quantitative Real-Time PCR for gene expression in thoracic aorta

The TaqMan Gene Expression Assays (Applied Biosystems Life Technologies Grand Island, NY, USA) used are shown (Table 1). No DNase treatment was performed as cDNA preparation was performed per the manufacturer's instructions. However, as an extra precaution and to ensure no DNA amplification, all TaqMan probes used were intron-spanning. After reverse transcription, cDNA (1 μL) underwent real-time PCR amplification with 10 μL 2X TaqProbe qPCR Mastermix-low ROX (BEQPCR-PL; MidSci St. Louis, MO, USA), 8 μL sterile water, 1 μL 20X TaqMan Gene Expression Assays probe [(Life Technologies Grand Island, NY, USA); see Table 1 for probe information]. The reactions were performed in triplicate using a 7500 Real Time PCR Machine (Applied Biosystems Grand Island, NY, USA) with the following cycles: 50°C-2min.; 95°C-1min.; 40 cycles of 95°C-15sec.; 60°C 1min. Genes analyzed were *Mmp2* (Mm00439498_m1), *Mmp7* (Mm00487724_m1), *Mmp9* (Mm00442991_m1), *Timp1* (Mm00441818_m1) and *Cybb* (*Nox2*; Mm01287743_m1). The average threshold cycles (C_T) for the cDNA were normalized to the expression level of beta-2 microglobulin (*B2m*; Mm00437762_m1). *B2m* is a gene involved in immune response as a member of the major histocompatability complex class 1, and is not involved in energy metabolism (Shertzer *et al*. 2013). *B2m* has been previously shown to be stable in high-fat diet induced oxidative stress in adipose tissue (Bailey-Downs *et al*. 2013), and in response to oxidative stress in the brain (Shertzer *et al*. 2013) and lung (Shimada *et al*. 2009). A C_T above 35 was considered to be not expressed, and measurements with standard deviations above 0.5 were discarded and repeated. Two LF male ART offspring were unable to be analyzed for gene expression due to complications during mRNA isolation. Five or six No ART controls were selected randomly from each group (HF males, LF males, HF females, LF females) to be used for gene expression analysis.

Statistical Analysis

The logarithms of offspring body weights were regressed on the ART effect (pregnancy through ART or not), diet effect (HF or LF), sex effect (female or male), time effect (weaning, 4^{th} week, 5^{th} week, 6^{th} week, and 7^{th} week since birth), as well as interaction effects including sex by diet, ART by time, and diet by time. Mothers are random effects in the model to capture the correlations between offspring that have the same mother. Since repeated measurements for the same offspring were taken at all time points, compound symmetry correlation structure was used to model the correlations among these observations. The model was constructed and chosen by biological considerations and diagnostic statistics. The main effects and interaction effects were all statistically significant at level 0.05. The compound symmetry correlation structure for modeling the repeated measurements on the same offspring was chosen for its highest likelihood and lowest Akaike information criterion (AIC), Bayesian information criterion (BIC) statistics. The studentized residual plot and normal quantile-quantile (QQ) plot suggest a consistent normality assumption, and do not indicate any obvious outliers.

At the time of sacrifice, correlations were computed and tested between the logarithms of body weights, intracellular ROS, extracellular ROS (2-OH-Et and Et), and the differences in cycle thresholds of *Mmp2, Mmp9, Timp1* and *Nox2*.

We also examined the associations between the diet, ART, and sex effects with MAP and gene expression. The significance of each of the three effects (diet, ART and sex) was tested

within fixed levels of the other two. For example, the association between diet and MAP (or gene expression) was tested within fixed levels of ART and sex.

Results

Effects of ART and diet on body weight from weaning to sacrifice

Increased offspring body weight has been observed separately in models of maternal obesity and ART (Ceelen *et al*. 2007, Samuelsson *et al*. 2008, Nelson *et al*. 2010, Belva *et al*. 2012, Morandi *et al*. 2012). We sought to determine whether the combination of ART and high fat diet consumption by the mothers and offspring would amplify the increase in body weight expected in the offspring. The use of ART resulted in offspring with increased body weight when compared to no ART controls (No ART; $p<0.0001$) at weaning (*i.e*. 22 days of age; Fig. 1A). However, this effect diminished over time as the No ART group began to catch up in growth and resulted in non-significant body weight differences at sacrifice (*i.e*. 55 ± 0.5 days; $p=0.1052$). Additionally, maternal and offspring consumption of a HF diet resulted in increased body weight of the offspring from weaning ($p<0.0001$) until sacrifice (Fig. 1B; $p<0.0001$). Male offspring weighed significantly more than females from weaning until sacrifice ($p<0.0001$; Fig. 1C). No effect of the interaction between diet and ART was observed in this study ($p>0.05$; data not shown). However, there was an interaction between diet and sex. Males in the HF group had a greater increase in body weight when compared to the LF males at sacrifice than the HF females did when compared to the LF females ($p<0.03$; 34.03 ± 0.71 g vs. 28.77 ± 0.41 g and 24.12 ± 0.48 g vs. 21.91 ± 0.37 g, respectively).

Effects of sex and diet on mean arterial pressure

Hypertension is another common risk factor for the development of CVD (WHO 2013b). We used mean arterial pressure (MAP; 1/3 systolic + 2/3 diastolic pressure) as a measure of blood pressure in the offspring. Overall, males had a higher MAP than females at sacrifice ($p=0.002$; Fig. 2A). This increased MAP was associated with an increased body weight at seven weeks of age in males when compared to females ($p<0.0001$; Fig. 1C). Further, MAP was positively correlated with body weight at sacrifice ($p<0.02$; Table 2). Diet also had an effect on offspring MAP ($p<0.05$) after taking into account ART and sex effects. When offspring consumed a HF diet after developing in a HF maternal environment, they had higher MAP than offspring that had been exposed to a LF diet throughout (Fig. 2B). We did not observe increased blood pressure due to ART ($p>0.05$, Supplemental Fig. 1).

Gene expression in response to diet and sex

Altered activities of MMP2, MMP7, MMP9, TIMP1 and NOX-derived ROS have been associated with CVD (Gomez *et al*. 1997, Lehoux *et al*. 2004, Wang *et al*. 2009). Further, MMP2 and 9 have been suggested to be involved in ROS-dependent vascular remodeling associated with hypertension (Martinez-Lemus *et al*. 2011). We examined gene expressions of *Mmp2*, *Mmp7*, *Mmp9*, *Timp1* and *Nox2* in the thoracic aorta of offspring from the different treatment groups to determine if these possible markers of cardiovascular health were affected by the two treatments alone or in combination. Offspring who were exposed to an obesogenic diet had lower expression of *Mmp9* and a tendency towards lower expression of *Mmp2* when compared to offspring in the LF group ($p<0.05$ and $p<0.1$, respectively; Fig. 3A and C). Further, males had decreased expression of *Mmp2* and the inhibitor *Timp1* ($p<0.05$ and $p<0.04$, respectively; Fig. 3B and D) when compared to females. No difference in expression of *Nox2* was observed between treatment groups ($p>0.05$, data not shown). Also, the use of ART did not show a significant difference in the expression of any of the genes assayed in this study ($p>0.05$, Supplemental Fig. 2). *Mmp7* expression was not detected in the thoracic aorta of the offspring from any treatment.

Several correlations with gene expression were observed in the offspring. The expression of all of the genes analyzed (*Mmp2*, *Mmp9*, *Timp1* and *Nox2*) were positively correlated with each other ($p<0.01$; Table 2). The differences in cycle thresholds of *Mmp2* also had a positive correlation and *Mmp9* tended to have a positive correlation with body weight at sacrifice ($p= 0.02$ and $p=0.06$, respectively; Table 2). Therefore, as the body weight increased, the expression of *Mmp2* decreased and *Mmp9* tended to decrease.

Effect of ART on ROS in offspring mesenteric resistance arteries

Previous research has shown increased oxidative stress, which can occur due to increased ROS, in obesity as well as with the use of ART (Chao *et al*. 2005, Torrens *et al*. 2012). We examined the levels of intracellular or extracellular ROS in mesenteric resistance arteries of the experimental offspring. Offspring produced by ART had increased intracellular ROS in mesenteric resistance arteries ($p=0.05$; 45.2 ± 2.47 and 37.67 ± 1.97, respectively; Fig. 4B–C2). There was no significant difference in intracellular ROS between the HF and LF groups ($p>0.05$; 41.96 ± 2.35 and 40.94 ± 2.27, respectively) or between the males and females ($p>0.05$; 39.57 ± 2.08 and 43.64 ± 2.57, respectively). Further, we did not observe a significant difference in the oxidation level of DHE outside the cells indicating that extracellular ROS did not differ in the mesenteric resistance arteries between treatment groups ($p>0.05$, data not shown).

2-OH-Et and Et as measured by HPLC in the extracellular solution containing DHE are a measure of extracellular superoxide (O_2^-) production and non-specific ROS production, respectively. Intracellular ROS did not correlate significantly with either extracellular 2-OH-Et or Et ($p>0.05$, data not shown). When extracellular 2-OH-Et was increased, Et was also increased ($p<0.001$; Table 2). Extracellular 2-OH-Et was negatively correlated with the differences in cycle threshold of *Mmp2*, *Mmp9*, *Timp1* and *Nox2* ($p<0.01$, $p<0.01$, $p<0.01$ and $p<0.02$, respectively; Table 2), meaning that as the expression of each of the four genes was increased, extracellular superoxide was also increased. Extracellular Et was negatively correlated with the differences in cycle threshold of all of the genes analyzed (Table 2). Also, there was a negative correlation between extracellular 2-OH-Et and MAP (Table 2).

Discussion

Both ART (Ceelen *et al*. 2007, Belva *et al*. 2012) and maternal diet-induced obesity (Samuelsson *et al*. 2008, Nelson *et al*. 2010, Morandi *et al*. 2012) have been shown to produce offspring with increased body weight or increased adiposity. Our study supported these previous findings, as both ART and diet affected offspring body weight. Maternal and offspring consumption of a HF diet resulted in offspring with higher body weight than the LF controls, and this effect persisted and increased from weaning (22 days) until sacrifice (55 ± 0.5 days). However, the effect of ART that we observed on increased body weight in the offspring decreased over time after weaning. This is similar to findings from a previous study (Scott *et al*. 2010), where female mouse offspring conceived using IVF had increased body weight at three weeks of age when compared to no ART controls, but not from four weeks of age until eight weeks of age. Further, one retrospective ART study in humans showed increases in child adiposity rather than body weight (Ceelen *et al*. 2007), while the other showed increases in adiposity and body weight (Belva *et al*. 2012). However, the study by Belva *et al*. (2012) involved intracytoplasmic sperm injection (ICSI) which is a more invasive ART procedure compared to those used in our study. Future studies examining the effect of ART on offspring should look at adiposity in addition to body weight and also the type of ART procedure used to further clarify this issue.

Maternal and offspring diet had a greater effect on body weight in the male offspring compared to females. Males from the HF group weighed significantly more when compared

to the LF males than the HF females did when compared to LF females. This finding is supported by previous research that exhibited pronounced adverse metabolic outcomes in males born to an obese mother (Torrens *et al*. 2012, Magliano *et al*. 2013). To our knowledge, no studies have previously been performed to examine the effect of ART and a HF developmental environment together on juvenile offspring body weight. Our study did not show a significant ART and diet interaction, suggesting that the adverse effects on offspring body weight from these two environments are not amplified by the combination of ART and HF diet consumption, at least at the age examined.

It has previously been reported that increased body weight can predispose an individual to adverse cardiovascular outcomes including hypertension and an increased risk for CVD (NIH 2012, Iguchi *et al*. 2013, Simoes-Silva *et al*. 2013). Data from our study support this previous research. First, males had increased body weight when compared to females from weaning until sacrifice, and this was accompanied by an increased MAP in males compared to females at sacrifice. The difference in MAP between males and females is also supported by previous research showing that estrogens can have a protective effect on blood pressure response [reviewed in (Xue *et al*. 2013)]. Further, MAP had a positive overall correlation with body weight at sacrifice, showing that individuals who were heavier had higher MAP.

Previous research has also shown increased blood pressure in offspring born to mothers consuming a high fat diet (Samuelsson *et al*. 2008, Torrens *et al*. 2012). Results from our study support these findings, as HF diet consumption (both by the dam and the offspring) resulted in increased MAP in the offspring.

In humans, an association has previously been made between the use of ART and increased systolic and diastolic blood pressure in children (Ceelen *et al*. 2008, Sakka *et al*. 2010). These retrospective studies involved children at ages from eight to 18 years old (Ceelen *et al*. 2008) and from four to 14 years old (Sakka *et al*. 2010) which we expect are comparable to the seven weeks of age juvenile mice that we studied. Further, an effect of ART on offspring blood pressure has also been observed in mice (Watkins *et al*. 2007). Our study, however, did not show increased MAP due to ART. There are several differences between the Watkins *et al*. (2007) work and ours that could partially explain the difference in results. For example, in our study we studied juvenile mice ($\sim$ 7 weeks of age) while they used older mice (*i.e*. 15 and 21 weeks of age). In addition, the strain of mice used varied between studies [NSA (CF1) females and B6D2F1/J males vs (CBA X C57/BL6)F1 females and MF1 males for our and their studies, respectively] and the embryo culture medium was different (Whitten's Medium vs T6 Medium, for our and their studies, respectively). Finally our measurement of MAP combines both systolic and diastolic pressure, while in the study by Watkins *et al*. (2007) only differences in systolic blood pressure were measured.

Interestingly, while offspring who were exposed to an obesogenic diet had increased MAP, they had lower expression of *Mmp2* and *Mmp9* when compared to offspring in the LF group. This is counterintuitive to previous studies that have suggested MMP2 and MMP9 to be involved in vascular remodeling associated with hypertension (Lehoux *et al*. 2004, Martinez-Lemus *et al*. 2011). However, in the study by Lehoux *et al*. (2004) MMP9 was shown to be involved in outward remodeling rather than inward remodeling (Lehoux *et al*. 2004), so increased MMP9 has been suggested to initially provide a compensatory response to increased pressure (Martinez-Lemus & Galinanes 2011). Therefore, it is possible that the decreased *Mmp9* expression found in the offspring with increased MAP is representative of a decreased ability of these offspring to compensate for their increased MAP. It should be noted that our interpretation of the results are based on measurements of signal for gene expression of the enzymes. Future experiments will determine whether protein expression and enzymatic activity align with our current findings.

Further, while males had increased MAP compared to females, they displayed decreased expression of *Mmp2*. However, they also displayed decreased expression of the inhibitor *Timp1*. Increased *Timp1* expression has previously been shown to inhibit the activity of MMP2 and MMP9 (Zacchigna *et al*. 2004); therefore, it is possible that decreased *Timp1* expression in the males is allowing for more MMP2 and MMP9 activity when compared to the females.

An ART effect was observed with levels of intracellular ROS in the offspring mesenteric resistance arteries. Superovulation, embryo culture and embryo transfer were used in this experiment in order to simulate three of the procedures commonly used in human ART. In this initial study, we chose to use Whitten's Medium to culture the embryos as this medium is known to be suboptimal for embryo development even though it is adequate to support development to full term (Ecker *et al*. 2004, Sommovilla *et al*. 2005). Future studies will determine if similar effects are observed with various culture conditions. Offspring who were conceived using ART had increased levels of ROS in their mesenteric resistance arteries when compared to the offspring who were conceived naturally. While this increase was not accompanied by a significant change in MAP, this could predispose the offspring to greater vascular dysfunction and remodeling, as increased levels of ROS have been associated with reduced bioavailability of NO and vascular remodeling (Katakam *et al*. 2005, Martinez-Lemus *et al*. 2011). The increased levels of intracellular ROS in the ART group also occurred without a significant change in *Nox2* expression. This could be an artifact of the different tissues used for ROS quantification and gene expression analysis. Alternatively, the increased ROS levels could be due to other producers of ROS [*i.e*. NOX1, NOX4, xanthine oxidase and nitric oxide synthase; (Cai *et al*. 2003, Bedard & Krause 2007, Demarco *et al*. 2010)]. Extracellular ROS levels were not significantly affected by any of the treatments.

We chose to study ROS levels in the resistance arteries, as the microvasculature is where most of the inward remodeling has been implicated in hypertension (Korsgaard *et al*. 1993). Due to limited amounts of tissue from the microvasculature, we performed gene expression analysis in the aorta. Dysfunction in the aorta has also been implicated in adverse cardiovascular health in rodents, and studies have been performed examining the MMPs and TIMPs in the aorta (Allaire *et al*. 1998, Khan *et al*. 2012). While we acknowledge that the aorta (a large conduit vessel) and the resistance arteries (resistance vessels) are not the same, and we cannot make strong causative conclusions in our findings between the two tissues, we can still use our findings as possible markers of adverse cardiovascular health in the offspring. Previous studies have also used both large conduit vessels and small resistance vessels to examine cardiovascular health in rodents (Beyer *et al*. 2008, Davidson *et al*. 2010, Sakurada *et al*. 2010, Agbor *et al*. 2012).

In summary, our study has shown an effect of ART on offspring body weight at weaning in a rodent model. We have also shown an effect of the use of ART on the level of ROS in mesenteric resistance arteries in the offspring. Maternal and offspring consumption of a HF diet resulted in increased body weight, MAP and misregulated gene expression in the offspring aortas. We further found a relationship between elevated extracellular ROS from mesenteric resistance arteries and increased gene expression of *Nox2*, *Mmp2*, *Mmp9*, and *Timp1* in the thoracic aorta. Knowledge is lacking on what effect the combination of ART and HF diet have on offspring body weight and cardiovascular health, but our data suggest that the two developmental environments do not have an additive effect on body weight, MAP, gene expression in thoracic aorta and ROS in mesenteric resistance arteries in juvenile mice. The experimental design used in the present study does not allow us to differentiate if the adverse cardiovascular outcomes observed were the result of exposure to an obesogenic diet prenatally or postnatally. Future research will examine this question.

Further, as CVD in humans often does not present until adulthood (Jousilahti *et al*. 1999), follow-up studies will also determine if an increased risk for adverse cardiovascular outcomes resulting from ART or obesogenic diet alone or in combination is evident later in life.

Supplementary Material

Refer to Web version on PubMed Central for supplementary material.

Acknowledgments

We would like to thank Matthew Sepúlveda from the Rivera laboratory for his valuable assistance with embryo transfer surgeries, and Guiling Zhao from the Martínez-Lemus laboratory for her help with isolation of the mesenteric resistance arteries.

Funding

ALS is funded by a Miller Fellowship granted by MU Division of Animal Sciences. RMR is funded by F21C. LAM-L is funded by grant R01 HL088105 from the National Heart, Lung and Blood Institute.

References

Agbor LN, Walsh MT, Boberg JR, Walker MK. Elevated blood pressure in cytochrome P4501A1 knockout mice is associated with reduced vasodilation to omega-3 polyunsaturated fatty acids. Toxicol Appl Pharmacol. 2012; 264:351–360. [PubMed: 22995157]

Allaire E, Forough R, Clowes M, Starcher B, Clowes AW. Local overexpression of TIMP-1 prevents aortic aneurysm degeneration and rupture in a rat model. J Clin Invest. 1998; 102:1413–1420. [PubMed: 9769334]

Bailey-Downs LC, Tucsek Z, Toth P, Sosnowska D, Gautam T, Sonntag WE, Csiszar A, Ungvari Z. Aging exacerbates obesity-induced oxidative stress and inflammation in perivascular adipose tissue in mice: a paracrine mechanism contributing to vascular redox dysregulation and inflammation. J Gerontol A Biol Sci Med Sci. 2013; 68:780–792. [PubMed: 23213032]

Bedard K, Krause KH. The NOX family of ROS-generating NADPH oxidases: physiology and pathophysiology. Physiol Rev. 2007; 87:245–313. [PubMed: 17237347]

Belva F, Painter R, Bonduelle M, Roelants M, Devroey P, De Schepper J. Are ICSI adolescents at risk for increased adiposity? Hum Reprod. 2012; 27:257–264. [PubMed: 22081314]

Beyer AM, Baumbach GL, Halabi CM, Modrick ML, Lynch CM, Gerhold TD, Ghoneim SM, de Lange WJ, Keen HL, Tsai YS, Maeda N, Sigmund CD, Faraci FM. Interference with PPARgamma signaling causes cerebral vascular dysfunction, hypertrophy, and remodeling. Hypertension. 2008; 51:867–871. [PubMed: 18285614]

Buettner GR. DETAPAC (DTPA), Aqueous Stock Solution. 2008

Cai H, Griendling KK, Harrison DG. The vascular NAD(P)H oxidases as therapeutic targets in cardiovascular diseases. Trends Pharmacol Sci. 2003; 24:471–478. [PubMed: 12967772]

Ceelen M, van Weissenbruch MM, Prein J, Smit JJ, Vermeiden JP, Spreeuwenberg M, van Leeuwen FE, Delemarre-van de Waal HA. Growth during infancy and early childhood in relation to blood pressure and body fat measures at age 8–18 years of IVF children and spontaneously conceived controls born to subfertile parents. Hum Reprod. 2009; 24:2788–2795. [PubMed: 19648588]

Ceelen M, van Weissenbruch MM, Roos JC, Vermeiden JP, van Leeuwen FE, Delemarre-van de Waal HA. Body composition in children and adolescents born after in vitro fertilization or spontaneous conception. J Clin Endocrinol Metab. 2007; 92:3417–3423. [PubMed: 17595253]

Ceelen M, van Weissenbruch MM, Vermeiden JP, van Leeuwen FE, Delemarre-van de Waal HA. Cardiometabolic differences in children born after in vitro fertilization: follow-up study. J Clin Endocrinol Metab. 2008; 93:1682–1688. [PubMed: 18285409]

Chao HT, Lee SY, Lee HM, Liao TL, Wei YH, Kao SH. Repeated ovarian stimulations induce oxidative damage and mitochondrial DNA mutations in mouse ovaries. Ann N Y Acad Sci. 2005; 1042:148–156. [PubMed: 15965057]

Davidson EP, Coppey LJ, Calcutt NA, Oltman CL, Yorek MA. Diet-induced obesity in Sprague-Dawley rats causes microvascular and neural dysfunction. Diabetes Metab Res Rev. 2010; 26:306–318. [PubMed: 20503263]

Demarco VG, Whaley-Connell AT, Sowers JR, Habibi J, Dellsperger KC. Contribution of oxidative stress to pulmonary arterial hypertension. World J Cardiol. 2010; 2:316–324. [PubMed: 21160609]

Ecker DJ, Stein P, Xu Z, Williams CJ, Kopf GS, Bilker WB, Abel T, Schultz RM. Long-term effects of culture of preimplantation mouse embryos on behavior. Proc Natl Acad Sci U S A. 2004; 101:1595–1600. [PubMed: 14747652]

Eppig JJ, Wigglesworth K, Pendola FL. The mammalian oocyte orchestrates the rate of ovarian follicular development. Proc Natl Acad Sci U S A. 2002; 99:2890–2894. [PubMed: 11867735]

Franco JG, Fernandes TP, Rocha CP, Calvino C, Pazos-Moura CC, Lisboa PC, Moura EG, Trevenzoli IH. Maternal high-fat diet induces obesity and adrenal and thyroid dysfunction in male rat offspring at weaning. J Physiol. 2012; 590:5503–5518. [PubMed: 22869015]

Gomez DE, Alonso DF, Yoshiji H, Thorgeirsson UP. Tissue inhibitors of metalloproteinases: structure, regulation and biological functions. Eur J Cell Biol. 1997; 74:111–122. [PubMed: 9352216]

Hales CNB, D JP. Type 2 (non-insulin-dependent) diabetes mellitus: the thrifty phenotype hypothesis. Diabetologia. 1992; 35:595–601. [PubMed: 1644236]

Hao L, Du M, Lopez-Campistrous A, Fernandez-Patron C. Agonist-induced activation of matrix metalloproteinase-7 promotes vasoconstriction through the epidermal growth factor-receptor pathway. Circ Res. 2004; 94:68–76. [PubMed: 14656925]

Iguchi A, Yamakage H, Tochiya M, Muranaka K, Sasaki Y, Kono S, Shimatsu A, Satoh-Asahara N. Effects of weight reduction therapy on obstructive sleep apnea syndrome and arterial stiffness in patients with obesity and metabolic syndrome. J Atheroscler Thromb. 2013 in press.

Jousilahti P, Vartiainen E, Tuomilehto J, Puska P. Sex, age, cardiovascular risk factors, and coronary heart disease: a prospective follow-up study of 14 786 middle-aged men and women in Finland. Circulation. 1999; 99:1165–1172. [PubMed: 10069784]

Kallen B, Finnstrom O, Lindam A, Nilsson E, Nygren KG, Otterblad PO. Congenital malformations in infants born after in vitro fertilization in Sweden. Birth Defects Res A Clin Mol Teratol. 2010; 88:137–143. [PubMed: 20063307]

Katakam PV, Tulbert CD, Snipes JA, Erdos B, Miller AW, Busija DW. Impaired insulin-induced vasodilation in small coronary arteries of Zucker obese rats is mediated by reactive oxygen species. Am J Physiol Heart Circ Physiol. 2005; 288:H854–H860. [PubMed: 15650157]

Kelsall CJ, Hoile SP, Irvine NA, Masoodi M, Torrens C, Lillycrop KA, Calder PC, Clough GF, Hanson MA, Burdge GC. Vascular dysfunction induced in offspring by maternal dietary fat involves altered arterial polyunsaturated fatty acid biosynthesis. PLoS One. 2012; 7:e34492. [PubMed: 22509311]

Khan JA, Abdul Rahman MN, Mazari FA, Shahin Y, Smith G, Madden L, Fagan MJ, Greenman J, McCollum PT, Chetter IC. Intraluminal thrombus has a selective influence on matrix metalloproteinases and their inhibitors (tissue inhibitors of matrix metalloproteinases) in the wall of abdominal aortic aneurysms. Ann Vasc Surg. 2012; 26:322–329. [PubMed: 22305865]

Korsgaard N, Aalkjaer C, Heagerty AM, Izzard AS, Mulvany MJ. Histology of subcutaneous small arteries from patients with essential hypertension. Hypertension. 1993; 22:523–526. [PubMed: 8406657]

Lawlor DA, Najman JM, Sterne J, Williams GM, Ebrahim S, Davey Smith G. Associations of parental, birth, and early life characteristics with systolic blood pressure at 5 years of age: findings from the Mater-University study of pregnancy and its outcomes. Circulation. 2004; 110:2417–2423. [PubMed: 15477400]

Lehoux S, Lemarie CA, Esposito B, Lijnen HR, Tedgui A. Pressure-induced matrix metalloproteinase-9 contributes to early hypertensive remodeling. Circulation. 2004; 109:1041–1047. [PubMed: 14967734]

Magliano DC, Bargut TC, de Carvalho SN, Aguila MB, Mandarim-de-Lacerda CA, Souza-Mello V. Peroxisome proliferator-activated receptors-alpha and gamma are targets to treat offspring from maternal diet-induced obesity in mice. PLoS One. 2013; 8:64258.

Martinez-Lemus LA, Galinanes EL. Matrix metalloproteinases and small artery remodeling. Drug Discov Today Dis Models. 2011; 8:21–28. [PubMed: 22125568]

Martinez-Lemus LA, Zhao G, Galinanes EL, Boone M. Inward remodeling of resistance arteries requires reactive oxygen species-dependent activation of matrix metalloproteinases. Am J Physiol Heart Circ Physiol. 2011; 300:H2005–H2015. [PubMed: 21460197]

Morandi A, Meyre D, Lobbens S, Kleinman K, Kaakinen M, Rifas-Shiman SL, Vatin V, Gaget S, Pouta A, Hartikainen AL, Laitinen J, Ruokonen A, Das S, Khan AA, Elliott P, Maffeis C, Gillman MW, Jarvelin MR, Froguel P. Estimation of newborn risk for child or adolescent obesity: lessons from longitudinal birth cohorts. PLoS One. 2012; 7:e49919. [PubMed: 23209618]

Nagy, AGM.; Vintersten, K.; Behringer, R. Manipulating the Mouse Embryo, A laboratory manual. third edition. Cold Spring Harbor Laboratory Press; 2003.

Negron-Perez VM, Echevarria FD, Huffman SR, Rivera RM. Determination of allelic expression of h19 in pre- and peri-implantation mouse embryos. Biol Reprod. 2013; 88:97. [PubMed: 23486912]

Nelson SM, Matthews P, Poston L. Maternal metabolism and obesity: modifiable determinants of pregnancy outcome. Hum Reprod Update. 2010; 16:255–275. [PubMed: 19966268]

NIH. Overweight and obesity statistics. 2012

Olson CK, Keppler-Noreuil KM, Romitti PA, Budelier WT, Ryan G, Sparks AET, Van Voorhis BJ. In vitro fertilization is associated with an increase in major birth defects. Fertil Steril. 2005; 84:1308–1315. [PubMed: 16275219]

Owusu-Ansah E, Yavari A, Banerjee U. A protocol for _in vivo_ detection of reactive oxygen species. 2008

Reefhuis J, Honein MA, Schieve LA, Correa A, Hobbs CA, Rasmussen SA. Assisted reproductive technology and major structural birth defects in the United States. Hum Reprod. 2009; 24:360–366. [PubMed: 19010807]

Rinaudo P, Schultz RM. Effects of embryo culture on global pattern of gene expression in preimplantation mouse embryos. Reproduction. 2004; 128:301–311. [PubMed: 15333781]

Robker RL. Evidence that obesity alters the quality of oocytes and embryos. Pathophysiology. 2008; 15:115–121. [PubMed: 18599275]

Rodrigues SF, Tran ED, Fortes ZB, Schmid-Schonbein GW. Matrix metalloproteinases cleave the beta2-adrenergic receptor in spontaneously hypertensive rats. Am J Physiol Heart Circ Physiol. 2010; 299:H25–H35. [PubMed: 20382857]

Sakka SD, Loutradis D, Kanaka-Gantenbein C, Margeli A, Papastamataki M, Papassotiriou I, Chrousos GP. Absence of insulin resistance and low-grade inflammation despite early metabolic syndrome manifestations in children born after in vitro fertilization. Fertil Steril. 2010; 94:1693–1699. [PubMed: 20045517]

Sakurada M, Yoshimoto T, Sekizawa N, Hirono Y, Suzuki N, Hirata Y. Vasculoprotective effect of cilostazol in aldosterone-induced hypertensive rats. Hypertens Res. 2010; 33:229–235. [PubMed: 20019701]

Samuelsson AM, Matthews PA, Argenton M, Christie MR, McConnell JM, Jansen EH, Piersma AH, Ozanne SE, Twinn DF, Remacle C, Rowlerson A, Poston L, Taylor PD. Diet-induced obesity in female mice leads to offspring hyperphagia, adiposity, hypertension, and insulin resistance: a novel murine model of developmental programming. Hypertension. 2008; 51:383–392. [PubMed: 18086952]

Samuelsson AM, Morris A, Igosheva N, Kirk SL, Pombo JM, Coen CW, Poston L, Taylor PD. Evidence for sympathetic origins of hypertension in juvenile offspring of obese rats. Hypertension. 2010; 55:76–82. [PubMed: 19901159]

Scherrer U, Rimoldi SF, Rexhaj E, Stuber T, Duplain H, Garcin S, de Marchi SF, Nicod P, Germond M, Allemann Y, Sartori C. Systemic and pulmonary vascular dysfunction in children conceived by assisted reproductive technologies. Circulation. 2012; 125:1890–1896. [PubMed: 22434595]

Scott KA, Yamazaki Y, Yamamoto M, Lin Y, Melhorn SJ, Krause EG, Woods SC, Yanagimachi R, Sakai RR, Tamashiro KL. Glucose parameters are altered in mouse offspring produced by assisted

reproductive technologies and somatic cell nuclear transfer. Biol Reprod. 2010; 83:220–227. [PubMed: 20445127]

Shertzer HG, Krishan M, Genter MB. Dietary whey protein stimulates mitochondrial activity and decreases oxidative stress in mouse female brain. Neurosci Lett. 2013; 548:159–164. [PubMed: 23748211]

Shimada I, Matsui K, Iida R, Tsubota E, Matsuki T. Time course of housekeeping gene expression changes in diffuse alveolar damage induced by hyperoxia exposure in mice. Leg Med (Tokyo). 2009; 11(Suppl 1):S151–S154. [PubMed: 19272828]

Simoes-Silva L, Moreira-Rodrigues M, Quelhas-Santos J, Fernandes-Cerqueira C, Pestana M, Soares-Silva I, Sampaio-Maia B. Intestinal and renal guanylin peptides system in hypertensive obese mice. Exp Biol Med (Maywood). 2013; 238:90–97. [PubMed: 23479768]

Siwik DA, Pagano PJ, Colucci WS. Oxidative stress regulates collagen synthesis and matrix metalloproteinase activity in cardiac fibroblasts. Am J Physiol Cell Physiol. 2001; 280:C53–C60. [PubMed: 11121376]

Sommovilla J, Bilker WB, Abel T, Schultz RM. Embryo culture does not affect the longevity of offspring in mice. Reproduction. 2005; 130:599–601. [PubMed: 16264090]

Torrens C, Ethirajan P, Bruce KD, Cagampang FR, Siow RC, Hanson MA, Byrne CD, Mann GE, Clough GF. Interaction between maternal and offspring diet to impair vascular function and oxidative balance in high fat fed male mice. PLoS One. 2012; 7:e50671. [PubMed: 23227196]

Wang X, Chow FL, Oka T, Hao L, Lopez-Campistrous A, Kelly S, Cooper S, Odenbach J, Finegan BA, Schulz R, Kassiri Z, Lopaschuk GD, Fernandez-Patron C. Matrix metalloproteinase-7 and ADAM-12 (a disintegrin and metalloproteinase-12) define a signaling axis in agonist-induced hypertension and cardiac hypertrophy. Circulation. 2009; 119:2480–2489. [PubMed: 19398663]

Watkins AJ, Platt D, Papenbrock T, Wilkins A, Eckert JJ, Kwong WY, Osmond C, Hanson M, Fleming TP. Mouse embryo culture induces changes in postnatal phenotype including raised systolic blood pressure. Proc Natl Acad Sci U S A. 2007; 104:5449–5454. [PubMed: 17372207]

Wen SW, Leader A, White RR, Leveille MC, Wilkie V, Zhou J, Walker MC. A comprehensive assessment of outcomes in pregnancies conceived by in vitro fertilization/intracytoplasmic sperm injection. Eur J Obstet Gynecol Reprod Biol. 2010; 150:160–165. [PubMed: 20207067]

WHO. Obesity and Overweight Fact Sheet. 2013a

WHO. Cardiovascular Diseases (CVDs) Fact Sheet. 2013b

Wikstrand MH, Niklasson A, Stromland K, Hellstrom A. Abnormal vessel morphology in boys born after intracytoplasmic sperm injection. Acta Paediatr. 2008; 97:1512–1517. [PubMed: 18754826]

Wildman RP, Mackey RH, Bostom A, Thompson T, Sutton-Tyrrell K. Measures of obesity are associated with vascular stiffness in young and older adults. Hypertension. 2003; 42:468–473. [PubMed: 12953016]

Xue B, Johnson AK, Hay M. Sex differences in angiotensin II- and aldosterone-induced hypertension: the central protective effects of estrogen. Am J Physiol Regul Integr Comp Physiol. 2013; 305:R459–R463. [PubMed: 23883676]

Yang Y, Estrada EY, Thompson JF, Liu W, Rosenberg GA. Matrix metalloproteinase-mediated disruption of tight junction proteins in cerebral vessels is reversed by synthetic matrix metalloproteinase inhibitor in focal ischemia in rat. J Cereb Blood Flow Metab. 2007; 27:697–709. [PubMed: 16850029]

Zacchigna S, Zentilin L, Morini M, Dell'Eva R, Noonan DM, Albini A, Giacca M. AAV-mediated gene transfer of tissue inhibitor of metalloproteinases-1 inhibits vascular tumor growth and angiogenesis in vivo. Cancer Gene Ther. 2004; 11:73–80. [PubMed: 14681728]

Zhang H, Wang ZW, Wu HB, Li Z, Li LC, Hu XP, Ren ZL, Li BJ, Hu ZP. Transforming growth factor-beta1 induces matrix metalloproteinase-9 expression in rat vascular smooth muscle cells via ROS-dependent ERK-NF-kappaB pathways. Mol Cell Biochem. 2013; 375:11–21. [PubMed: 23275087]

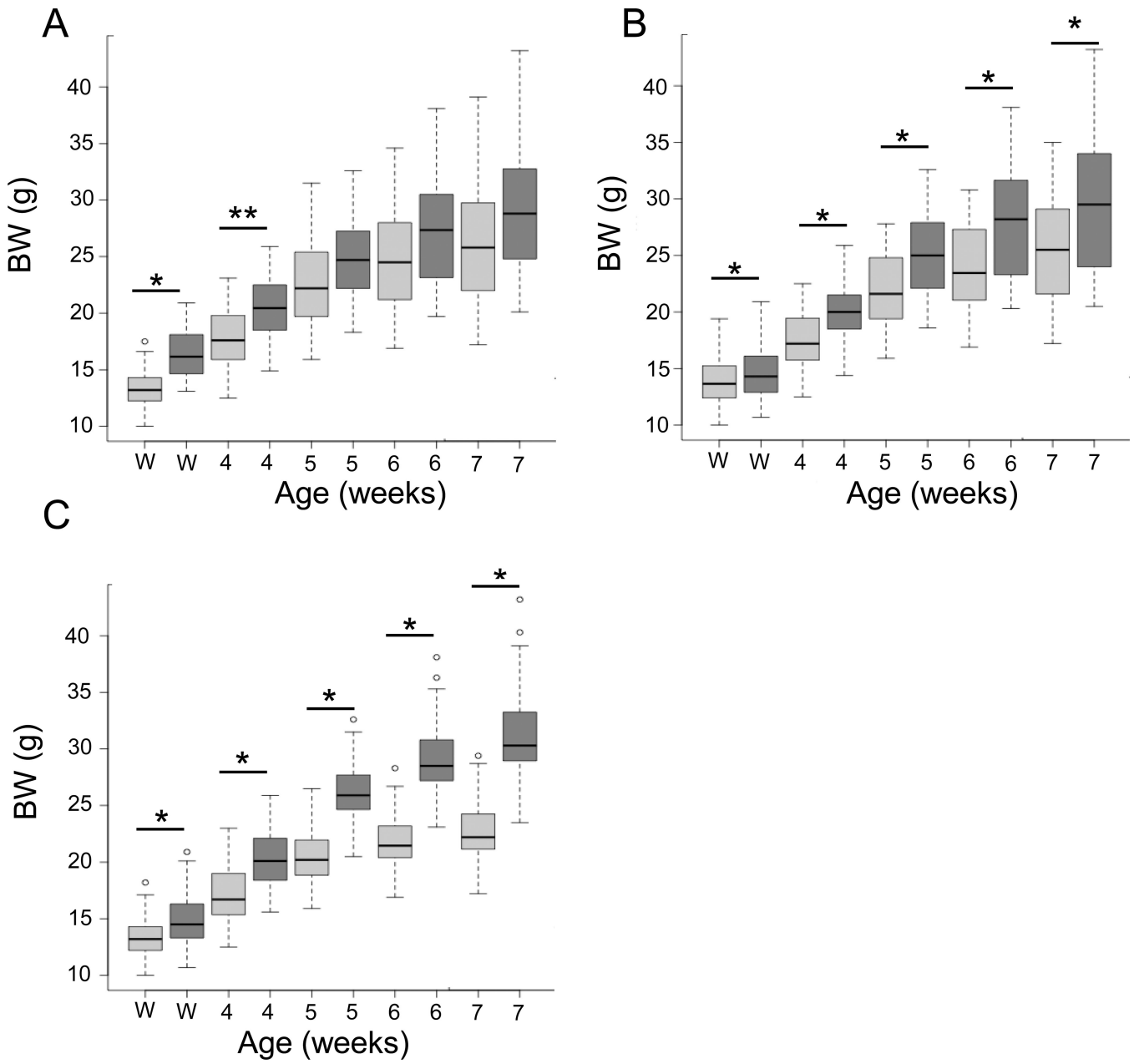

Figure 1. Effects of ART, diet and sex on mouse offspring body weight from weaning until seven weeks of age

A. Body weights for all offspring conceived by natural conception (No ART; n=87; light grey bars) or with the use of ART (ART; n=36; dark grey bars). **B**. Body weights for all offspring conceived by from mothers consuming a maintenance chow (LF; n=68; light grey bars) or a diet containing 24% fat and 17.5% high fructose corn syrup (HF; n=55; dark grey bars). **C**. Body weights of females (n=60; light grey bars) and males (n= 63; dark grey bars). Comparisons were made at weaning (22 days), week 4 (26 days), week 5 (33 days), week 6 (40 days) and week 7 (47 days). The middle bar in a box shows the median (50%) body weight. The upper and lower borders of a box show the 1st and 3rd quartiles (25% and 75%, respectively) of a group body weight. The bars above or below the dash lines mark the body weights that are 2.5 times of a quartile away from the median. Dots outside of bars are even

further away from the median. ART = assisted reproductive technologies. BW = body weight. Solid black lines with asterisks above are used to demarcate statistical differences between groups at given times after birth. * = $p<0.0001$, ** = $p<0.05$.

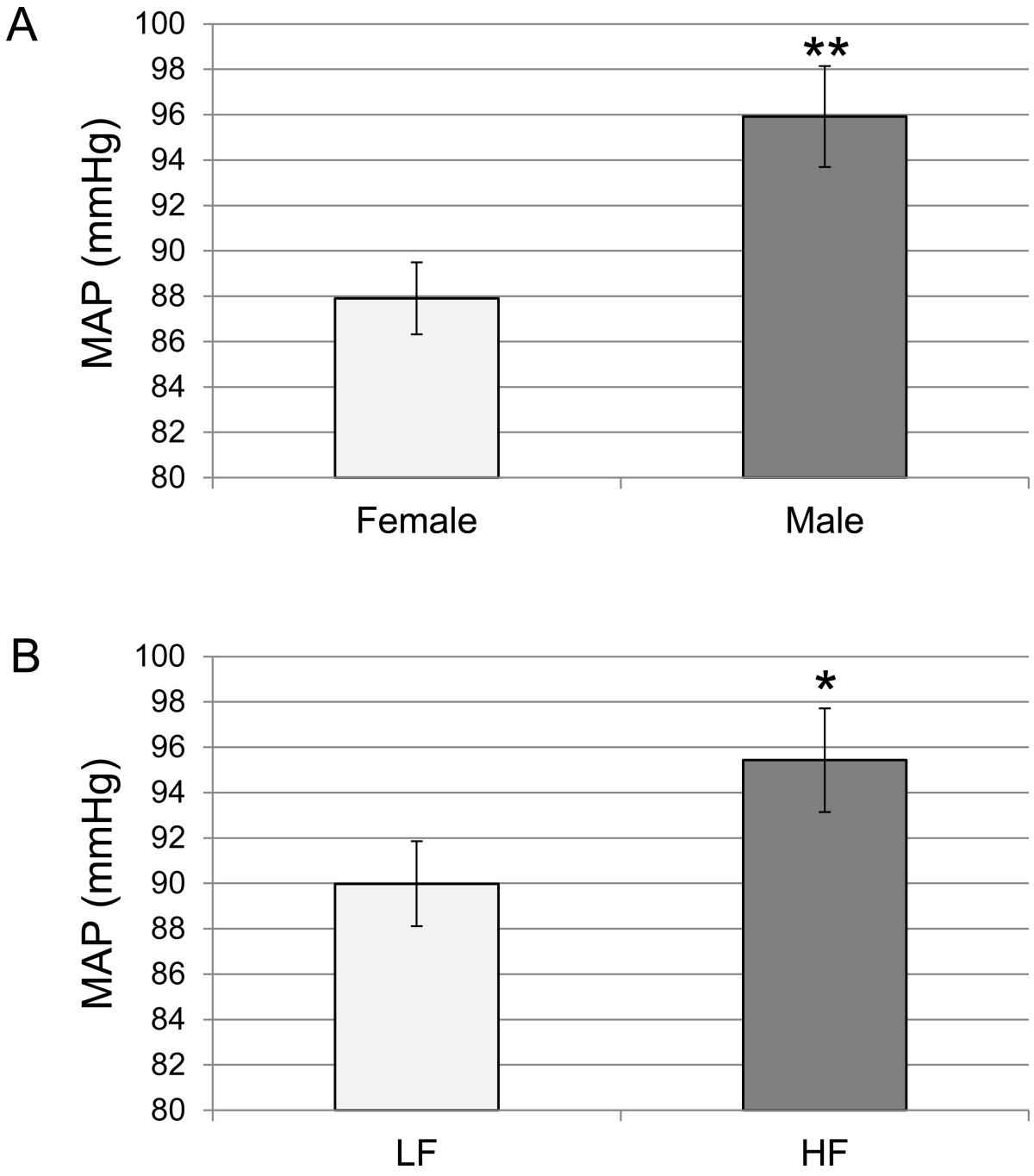

Figure 2. Mean arterial pressure (MAP) in offspring at sacrifice

Carotid artery catheterization was performed to measure MAP as a representation of blood pressure in the offspring immediately prior to sacrifice (55 ± 0.5 days). A. MAP in female (n=29) and males (n=33), offspring. **B**. MAP in LF (n=37) and HF (n=25) offspring. The bars represent the mean ± the S.E.M. LF=maternal and offspring consumption of a maintenance chow. HF=maternal and offspring consumption of a diet containing 24% fat and 17.5% high fructose corn syrup. *p<0.05. **p<0.01.

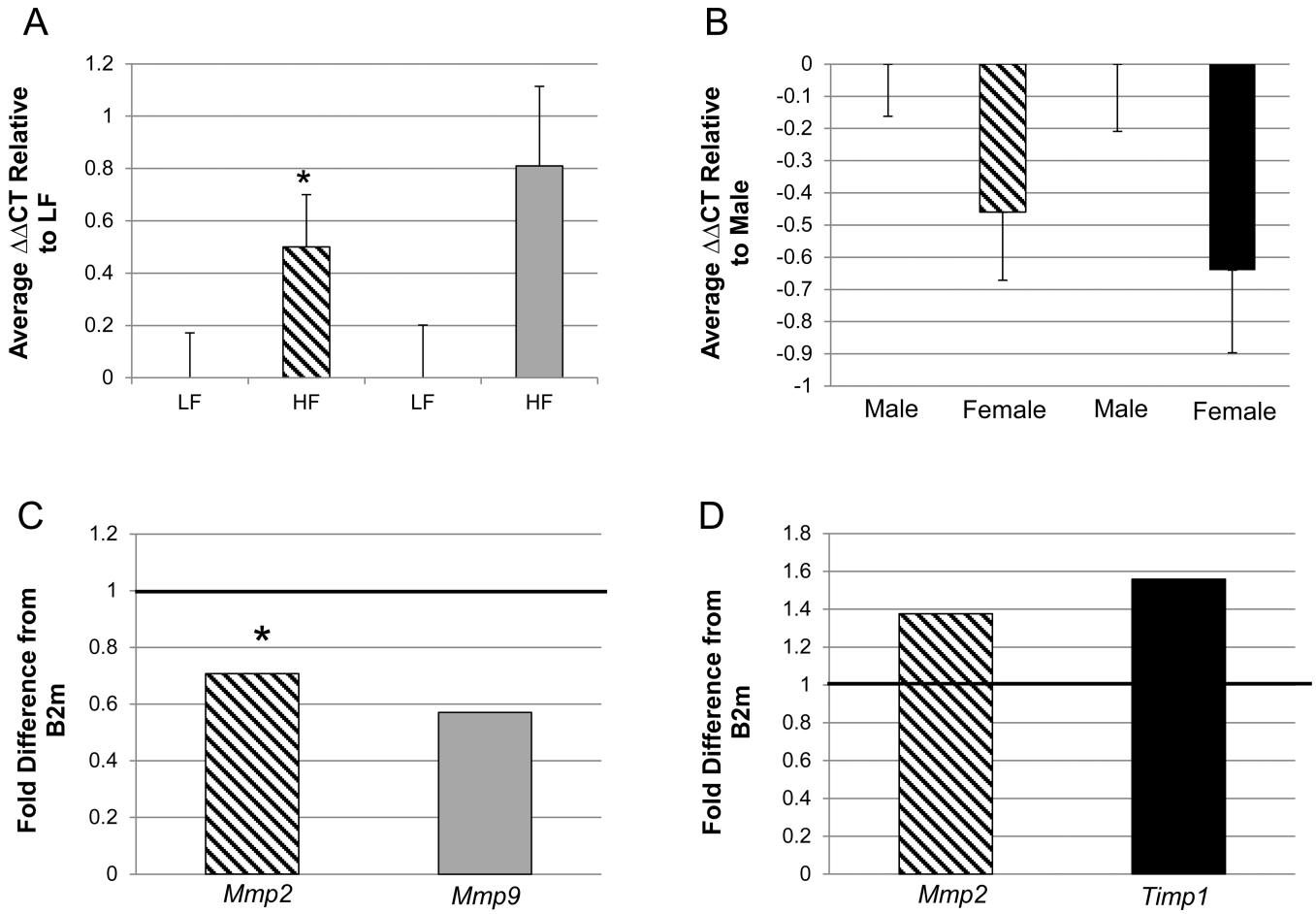

Figure 3. Quantitative RT-PCR assessment of the expression of genes potentially involved in inward remodeling in offspring thoracic aortas

All gene expressions were normalized to the expression of *B2m* (ΔC_T) and then averaged within the respective groups. **A**. The relative difference in cycle thresholds (ΔΔCT) between the HF and LF treatment groups for *Mmp2* and *Mmp9*. **B**. The relative difference ΔΔCT between females and males for Mmp2 and *Timp1*. The error bars represent the S.E.M. The fold differences between treatments groups for each gene analyzed were then calculated. **C** = fold difference calculation of data presented in **A. D** = fold difference calculation of data presented in **B**. The solid black line across "1" demarcates "LF" for the two bars in **C** (diet effect) and "males" in **D** (sex effect). *Mmp2* = diagonal line bar; *Mmp9* = gray bar; *Timp1* = black bar. *MMp2* - HF vs. LF, females vs. males; n=24 and 29, n=24 and 29, respectively. *Mmp9* - HF vs. LF n=24 and 29, respectively. *Timp1* - females vs. males; n=24 and 29, respectively. All differences are significant at $p<0.05$, except for the asterisk (*) which represents a trend at $p<0.1$. LF=consumption of maintenance chow by mothers and offspring. HF=maternal and offspring consumption of a diet with 24% fat and 17.5% high fructose corn syrup. ΔC_T = change in cycle threshold. *B2m*= beta 2-microglobulin.

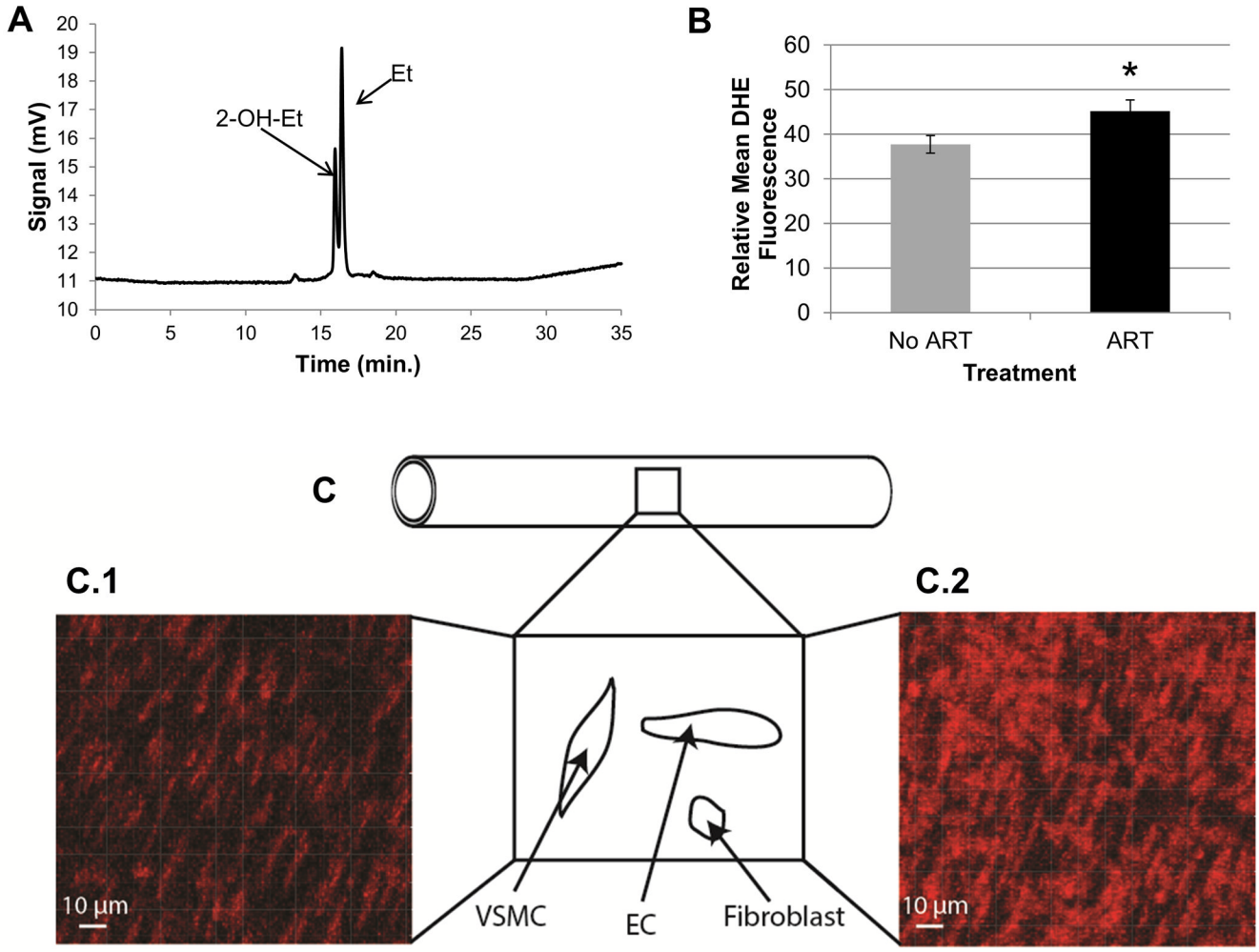

Figure 4. Detection of extracellular and intracellular ROS in mesenteric resistance arteries of offspring

A. Two fluorescent byproducts of dihydroethidium (DHE) were detected by high performance liquid chromatography (HPLC) in offspring (55 ± 0.5 days) mesenteric resistance arteries. Resistance arteries were incubated with 50 µM DHE for one hour. 2-hydroxyethidium (2-OH-Et; specific byproduct of superoxide and DHE) eluted at 16.19 ± 0.03 min and the ethidium (Et; less specific byproduct) eluted at 16.61 ± 0.03 min. Areas under each curve were determined using the Empower program (Waters, Build #1154) and were normalized to the concentration of protein in each vessel before comparisons between treatments. Protein amounts were with a Micro BCA™ Protein Assay Kit. **B**. Determination of levels of intracellular ROS in offspring mesenteric resistance arteries using confocal microscopy for relative DHE fluorescence. Intracellular DHE fluorescence (red) was measured by confocal microscopy. Gain was set at 800 V. Data represent the group average ± S.E.M. of DHE fluorescence over the average of two areas of the mesenteric resistance arteries for offspring conceived naturally (No ART; gray, n=32) or with the use of ART (ART; black, n=31). **C**. Shown is a diagrammatic representation of a resistance artery indicating that a portion of the middle section of the vessel was flattened and the vascular wall imaged using confocal microscopy to detect DHE-dependent fluorescence. Within the wall nuclei of different cells (i.e., VSMC=vascular smooth muscle cells, EC=endothelial cells, and fibroblasts) bind to the dye and highlight its fluorescence intensity. Notice that the

nuclei for different cells have specific morphologies and spatial orientations. The micrograph of a longitudinal section of a mesenteric resistance artery from a naturally conceived LF male is shown in **C.1**, and an ART conceived LF male in **C.2**. Red fluorescence results from the oxidation of DHE. Fluorescence was quantified with the Imaris 7.6.1 software. ART = assisted reproductive technologies. DHE = dihydroethidium. ROS = reactive oxygen species. *p=0.056.

Table 1

TaqMan probes used for quantitative RT-PCR analyses in mouse thoracic aorta

Name (NCBI accession no.)	Sequence	Amplicon Length (bp)
B2m (NM_009735.3)	CGGCCTGTATGCTATCCAGAAAACC	77
Mmp2 (NM_008610.2)	ACCAGATCACATACAGGATCATTGG	62
Mmp7 (NM_010810.4)	GGAACAGGCTCAGAATTATCTTAGA	128
Mmp9 (NM_013599.2)	TCCAGTACCAAGACAAAGCCTATTT	76
Timp1 (NM_001044384.1NM_011593.2)	CTGCAACTCGGACCTGGTCATAAGG	90
Cybb (NM_007807.4)	AGTGAACACCCTAACACCACAATAG	63

NCBI= National Center for Biotechnology Information. No.= number. Bp= base pairs.

Table 2

Table of significant correlations between measurements in mouse offspring.

	MMP9	*Timp1*	*Nox2*	2-OH-Et	Et	SacBW	MAP
MMP2	**0.717** **< 0.001** **53**	**0.742** **<0.001** **53**	**0.374** **0.006** **53**	**−0.364** **0.008** **52**	**−0.280** **0.045** **52**	**0.317** **0.021** **53**	0.225 0.112 51
MMP9		**0.634** **< 0.001** **53**	**0.549** **< 0.001** **53**	**−0.387** **0.005** **52**	**−0.363** **0.008** **52**	0.259 0.061 53	0.111 0.439 51
Timp1			**0.479** **<0.001** **53**	**−0.420** **0.002** **52**	**−0.293** **0.035** **52**	0.178 0.203 53	0.157 0.274 51
Nox2				**−0.338** **0.014** **52**	−0.258 0.065 52	−0.007 0.954 53	0.223 0.116 51
2-OH-Et					**0.848** **< 0.001** **67**	0.009 0.939 67	**−0.264** **0.04** **61**
Et						0.095 0.444 67	−0.136 0.294 61
SacBW							**0.295** **0.020** **62**

The logarithms of the ΔCT for matrix metalloproteinase 2 and 9 (Mmp2 and 9), tissue inhibitor of matrix metalloproteinase 1 (Timp1), and NADPH Oxidase 2 (Nox2) expression in thoracic aorta, extracellular 2-hydroxyethidium (2-OH-Et) and ethidium (ET) in mesenteric arterioles, body weight at sacrifice (SacBW) and mean arterial pressure (MAP) were compared using correlational analysis. The values in each cell from top to bottom represent the Pearson correlation coefficient, p-value and number of measurements; respectively. Boldface = significance at $p<0.05$. ΔCT= difference in cycle threshold.